

Investigate the Structural Response of Ultra High Performance Concrete Column under the High Explosion

Viet-Chinh Mai^{@*}, Xuan-Bach Luu[@], Cong-Binh Dao[#], and Dinh-Viet Le¹

[@]Department of Civil Engineering, Kumoh National Institute of Technology, Gumi - 39177, South Korea

[#]Institute of Techniques for Special Engineering, Le Quy Don Technical University, Ha Noi, Viet Nam

¹Department of Civil Environmental and Railroad Engineering, PaiChai University, Daejeon, South Korea

*E-mail: maivietchinh@lqdtu.edu.vn

ABSTRACT

Most of the structures that are damaged by an explosion are not initially designed to resist this kind of load. In the overall structure of any building, columns play an important role to prevent the collapse of frame structure under blast impact. Hence, the main concept in the blast resistance design of the building is to strengthen the blast loading capacity of the column. In the present study, the dynamic analysis and numerical model of Ultra High Performance Concrete (UHPC) column under high explosive load, is presented. Based on the Johnson Holmquist 2 damage model and the subroutine in the ABAQUS platform, a total of twenty numerical models of the UHPC column were calculated. The objective of the article is to investigate the structural response of the UHPC column and locate the most vulnerable scenarios to propose necessary recommendations for the UHPC column in the blast resistance design. The input parameters, including the effect of various shapes of cross-section, scaled distance, steel reinforcement ratio, and cross-section area, are analysed to have a better understanding of the UHPC column subjected to the blast load. Based on the results of this study, the UHPC circular column was demonstrated to achieve great blast resistance capacity. Details of the numerical data, and the discussion on the important results, are also provided in this paper.

Keywords: Column; Ultra high performance concrete; Explosion; Numerical model; Johnson-Holmquist 2 model; Failure

1. INTRODUCTION

Ongoing different accidental or intentional events related to the explosions lead to loss of lives as well as the infrastructure, thereby increasing the importance of analysis for structures under blast loading¹. Hazard assessment and dynamic response investigation of structures under a blast is an interesting topic that always attracts the attention of researchers. One of the important measures to resist blast loading and reduce damage to structures is to study material characteristics and their relationship with structural design².

A large number of concrete structural members are constructed as a part of the urban environment, as well as a part of the infrastructure. Based on fracture mechanics, conventional concrete is known as a typical brittle material and its dynamic behaviour depends on the strain rate which has a significant impact on the evolution of damage. In the blast resistance design, high energy-absorbing capability material is a vital factor, implying that the structures with large plastic deformation capacities are therefore desirable. However, conventional concrete with its brittle characteristic does not fulfill this requirement³. In the past decades, researchers have focused on developing new concrete composites, such as UHPC. UHPC study is implemented widely and 200MPa of

compressive strength or even over 200MPa can be obtained with advanced production technology⁴⁻⁹. It has commonly been assumed that the enhancing compressive strength of concrete may cause higher brittle property. Nevertheless, the demanding requirements of the component and the proper content addition of steel fiber into the UHPC mix have a positive effect on its ductility. Compared to plain concrete material, UHPC shows a greater energy-absorbing capability¹⁰⁻¹².

Most of the buildings adopt columns as the main support¹³. Therefore, studying the UHPC column subjected to blast loading, is importantly meaningful in the blast loading resistance design of the frame structure. Fujikura & Bruneau¹⁴ conducted the tests on quarter-scale reinforced concrete bridge columns subjected to the close-in explosion without the application of axial load. After the test, the seismic resistance columns did not show ductile response but experienced brittle failure due to direct shear at the base. Williamson¹⁵, *et al.* investigated the structural behaviour of a total of 10 reinforced concrete bridge columns under blast loading. Input parameters including steel bar ratio, column aspect ratio, and standoff distance were considered. The obtained results revealed that compared to the non-seismic resistance design, the seismic design column shows a more significant performance under blast loading. Besides, the noteworthy results of structural behaviour for conventional concrete columns under the blast can be found in the literature of Ref¹⁶⁻¹⁹, etc. For UHPC material, only a

few experiments related to the column subjected to blast were performed. Astarioglu & Krauthammer²⁰ used the simulation method to study the blast resistance of UHPC column under blast load. Using the SDOF approach, the effect of material, boundary condition, and the axial load was considered. They concluded that compared to normal concrete, UHPC columns reduced nearly 30% of deflection. Nine compact-reinforced composite (CRC) columns and a proprietary UHPC column using a shock-tube, were tested by Aoude²¹, *et al.* They reveal that fiber and steel reinforcement can impact the effectiveness of the column whereas UHPC contributes to the improvement in damage tolerance. Recently, Su²², *et al.* conduct experiments to investigate the response of columns made of UHPC material with nanoparticles under blast action. Based on the results, they hold the view that such material possesses great blast resistance capacity. Obtained results from these studies reveal that UHPC columns are found to greatly reduce maximum displacement, residual displacement as well as demonstrate the potential of UHPC material to strengthen the blast resistance capacity of the structure.

Due to the strict requirements for blast experiment, extensive testing regimes will entail time and high cost that constraint the application of UHPC in real life structures. Nowadays, the FEM has become a crucial tool in engineering research, particularly for blast loading simulation. This study presents the simulation model, using the JH2 approach to investigate the dynamic response of the UHPC columns under blast action.

2. MATERIAL AND METHOD

In terms of the existing dynamic constitutive model, the JH2 model represents a good compromise between complicated requirements of dynamic analysis and accuracy for large-scale computations. In the JH2 model, each state possesses its strength equation in which describes the relationship of normalised pressure against equivalent stress. The detailed mathematical formulation of the JH2 model can be found in studies of Holmquist^{23,24}, *et al.* This section only presents the basic equations of the JH2 model.

In the JH2 model, the strength is determined by the equivalent stress as:

$$\sigma^* = \sigma_i^* - D(\sigma_i^* - \sigma_f^*) \quad (1)$$

where: D is a scalar damage parameter. σ_i^* , σ_f^* define the normalised intact equivalent stress and the normalised fractured equivalent stress, which can be express in the equations:

$$\sigma_i^* = A(P^* + T^*)^N / (1 + C \ln \varepsilon) \quad (2)$$

$$\sigma_f^* = B(P^*)^M (1 + C \ln \varepsilon) \quad (3)$$

A ; B ; C ; M , and N , are the material parameters. ε is the strain rate. The normalised pressure P^* and maximum tensile hydrostatic pressure T^* can be written as:

$$P^* = P / P_{HEL} \quad (4)$$

$$T^* = T / T_{HEL} \quad (5)$$

P and T are the actual pressure and maximum tensile pressure, respectively. P_{HEL} is the pressure at Hugoniot elastic limit (HEL).

The damage propagation in the JH2 model with the plastic strain is expressed as:

$$D = \sum \frac{\Delta \varepsilon^{-pl}}{\varepsilon_f^{-pl}(P)} \quad (6)$$

$$\varepsilon_f^{-pl} = D_1(P^* + T^*)^{D_2} \quad (7)$$

D_1 , D_2 denote the constants of the material. $\Delta \varepsilon^{-pl}$ represents the increment of the plastic strain, and $\varepsilon_f^{-pl}(P)$ is the equivalent plastic strain at failure state.

Although the JH2 model has not been implemented in ABAQUS for numerical simulations yet, however, a designed subroutine can provide suitable variables according to user requirements. This subroutine is to describe the characteristics and the constitutive law of UHPC material. The validation of the proposed model is discussed in the following section.

3. RESULTS AND DISCUSSION

3.1 Verification of the Simulation Model

It is necessary to validate the proposed model to verify the accuracy of the simulation and the corresponding results. The important aspects to be verified including modelling blast dynamics and non-linear response of the structure. According to the JH2 approach, Mai²⁵, *et al.* used numerical simulation to investigate the dynamic behaviour of UHPC panels under high explosion. The analysis results in comparison to the test of Mao²⁵, *et al.* demonstrated the accuracy of the supposed model. Detailed results are presented in the study of Mai²⁶, *et al.* In the present study, a subroutine integrated on the Abaqus software, using the JH2 approach, was designed to simulate the UHPC column under blast load. Four UHPC columns under different loading conditions such as TNT equivalent charge weight, axial load, were analysed. The obtained results are compared to the experimental data of Xu²⁷, *et al.* The material parameters and details of the UHPC columns are listed in Tables 1(a), 1(b)^{28,29}. The geometry of the UHPC column, experimental model, and 3D simulation model in ABAQUS are shown in Figs. 1(a), 1(b), 1(c). In the numerical simulation, the three-dimensional eight-node reduced integration (C3D8R) element type is adopted for the concrete element. C3D8R element has eight nodes with three degrees of freedom, three translations in x, y, and z directions. C3D8R element can be used for 3D modelling of solids with or without reinforcement and it is capable of accounting for cracking of concrete in tension, crushing of concrete in compression, creep, and large strains. 3D linear truss (T3D2) elements are used to model the steel bar. This element is to model slender, line-like components with only axial loading along with the element.

The CONWEP (Conventional Weapons Effects) blast loading model, which is based upon the results of tests and the effects of the blast, was selected in this study. This model contains both positive and negative phases on a user-defined amount of TNT at a given distance from the explosion source^{30,31}. Figs. 1(d)-1(g) show blast pressure during time history and the energy result of blast simulation. The blast overpressure, P_{so} , for a high explosion of 35kg TNT and 17.5kg TNT equivalent, is 38.27MPa and 20.54MPa, respectively. Hourglass energy

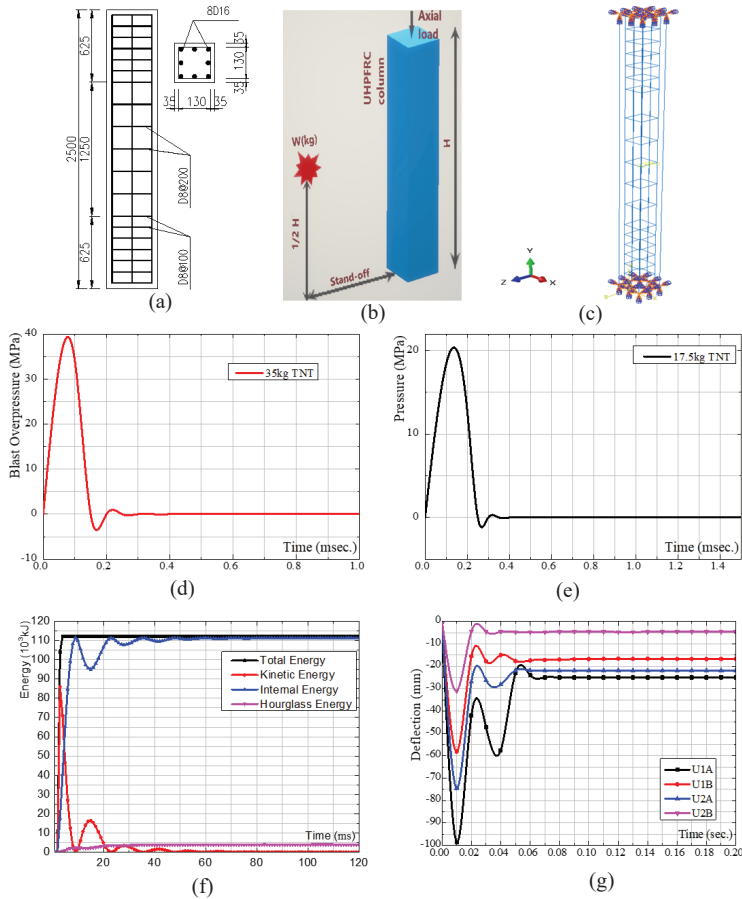


Figure 1. (a) Geometry of UHPC column in the test of Xu, (b) Test model, (c) 3D model in Abaqus, (d, e) blast wave pressure-time history, (f) Energy result from blast simulation, and (g) Deflection result after the blast.

represents artificial strain energy for the whole model (ALLAE). The smaller value of hourglass energy indicates the accurate simulation result, and this value must be less than 10% of the internal energy³². In the 35 kg TNT equivalent blast, the hourglass energy is 3.9 kJ, which is 3.5% of the largest internal energy (111.5 kJ). In the 17.5 kg TNT equivalent explosion, 0.6 kJ hourglass energy value is 1.1% compared to internal energy (50.48 kJ). These hourglass energy values demonstrated the accuracy of the simulation result. Furthermore, Table 1(c) and Fig. 1(g) show the value of maximum deflection and permanent deflection at the mid-span of the column after the blast. An agreement between the experimental and finite element results are obtained except for permanent deflection of column U1A. This discrepancy could be attributed to the real factors in a blast test such as charge weight, environmental

condition, specimens, etc. Therefore, less than a 10% disparity between simulation results and the test result is acceptable.

3.2 Parametric Studies

3.2.1 Shape Parameter of Column

Effect of shape parameter on the structural behaviour of UHPC columns under blast loading, including square cross-section, octagonal section, and circular section, is investigated. A 500×500 mm square column is the controlled model. By equating the volume of this square column, the cross-section of the octagonal and circular column can be obtained. These columns contain 1% steel reinforcement bar volume under stand-off distance of the detonation is 1.5m. The applied explosive charge weight is 50 kG TNT equivalent. An axial load of 7100 KN (20%

Table 1. (a) Material parameters for UHPC, (b) Details of UHPC columns in the test of Xu²⁷, et al. , and (c) Deflection result after the blast

(a)		
Variable	Description	UHPC
ρ (kg/m ³)	Density	2550
f_c (MPa)	Compressive strength	158
f_t (MPa)	Tensile strength	8.4
G (MPa)	Shear Modulus	33200
A	Failure Surface Constant	0.79
B	Failure Surface Constant	0.79
C	Failure Surface Constant	0.007
ϵ^*_0	The reference strain rate	1
S_{max}	Material Constant	12.5
D_1/D_2	Material Constant	0.05/1
P_{HEL}	The pressure at the HEL	19
K_1 (MPa)	Equation of State Constant	8.5
K_2 (MPa)	Equation of State Constant	17.1
K_3 (MPa)	Equation of State Constant	20.8

(b)			
Column	TNT equivalent (kg)	Axial load (kN)	Stand-off distance (m)
U1A	35	0	1.5
U1B	17.5	0	1.5
U2A	35	1000	1.5
U2B	17.5	1000	1.5

(c)

Col.	Max. deflection (1)	Max. deflection (2)	Disparity %	Permanent deflection (1)	Permanent deflection (2)	Disparity %
U1A	-	98.54 mm	-	21 mm	24.95 mm	15.8
U1B	63 mm	58.10 mm	-7.7	18.5 mm	16.7 mm	-9.7
U2A	68 mm	74.46 mm	8.6	23 mm	21.83 mm	-5.1
U2B	29.3 mm	30.9 mm	5.5	4 mm	4.28 mm	7

Note: (1)- Xu’s test; (2)- Simulation’s result

of load capacity) is enabled to act on the head of all columns. Details of these columns are shown in Figs. 2(a), 2(b), 2(c).

Figure 2(c) depicts the maximum deflection of the UHPC column for various cross-section after the blast. Square, octagonal, and circular cross-section exhibit the maximum deflection at the mid-span of 32.59 mm, 21.37 mm, and 14.72 mm, respectively. Both maximum deflection and permanent deflection, the circular cross-section show the smallest value compared to the rest. A possible explanation for these results may be the effect of peak reflected pressure at the exposed edge. Shapes with multiple angles and edges can reduce this pressure, resulting in a decrease in blast impact on the surface of the column. Therefore, the UHPC circular column shows considerable resistance towards blast loading. Moreover, the smaller permanent deflection reveals the rapid

Table 2. Damage state of UHPC column after the explosion (percentage by volume)

Cross-section	Standoff distance (m)	Light damage	Moderate damage	Severe damage	Collapse
Square Sec.	1.5	14.6%	11.2%	4.8%	//
Octagonal Sec.	1.5	18.7%	16.3%	7.2%	//
Circular Sec.	1.5	22.1%	19.5%	11.4%	//

dissipation of reflected pressure on the surface of the circular column. Similarly, in Fig. 2(e), the observed strain in the UHPC element of circular column (2184.6 μs) is remarkably less than the octagonal column (3482.35 μs) and square column (5801.39 μs). The damage state of the UHPC column for various cross-sections is shown in Figs. 2(f), 2(g), 2(h) and Table 2. It can be seen that the damage of the column increases as the cross-section changes from the circular shape to the octagonal and square shape. UHPC square section column undergoes 11.4% severe damage by volume compared to 7.2% of the octagonal column and 4.8% of the circular column. These results would seem to suggest that the UHPC column with square cross-section should not be used in the blast-resistant design. On the contrary, the circular cross-section is the best design for the column subjected to blast load in terms of reducing deformation and damage.

3.2.2 Scaled Distance Parameter

Dynamic response of a 500 × 500 mm UHPC square column with 1% steel reinforcement bar volume is studied under blast loading of 50kg TNT equivalent. The axial load of this UHPC column is 7100 KN (20% of load capacity). In a blast, the relationship between the stand-off distance R and the charge weight W can be expressed in the equation:

$$Z = R / W^{1/3} \tag{8}$$

Blast loading conditions for each regime can be defined by the value the scaled distance of Z, which is shown in Table 3(a)³³. In the present study, the model is calculated in four cases of scaled distance (Table 3(b)), corresponding to the close-in regime, near field, and the far-field regime. Structural behaviour of UHPC columns after the explosion is shown in Fig. 3. The graph shows that there has been

Table 3. (a) The response regime in the Smith³³, *et al.* and (b) Scaled distance for this study

(a)		
Scaled distance	Z (m/kg ^{1/3})	
Close in	Z < 1.19	
Near field	1.19 < Z < 3.97	
Far field	3.97 < Z	
(b)		
R (m)	Z (m/kg ^{1/3})	Scaled distance
1	0.27	Close in
1.5	0.41	Close in
4.5	1.22	Near field
14.7	3.98	Far field

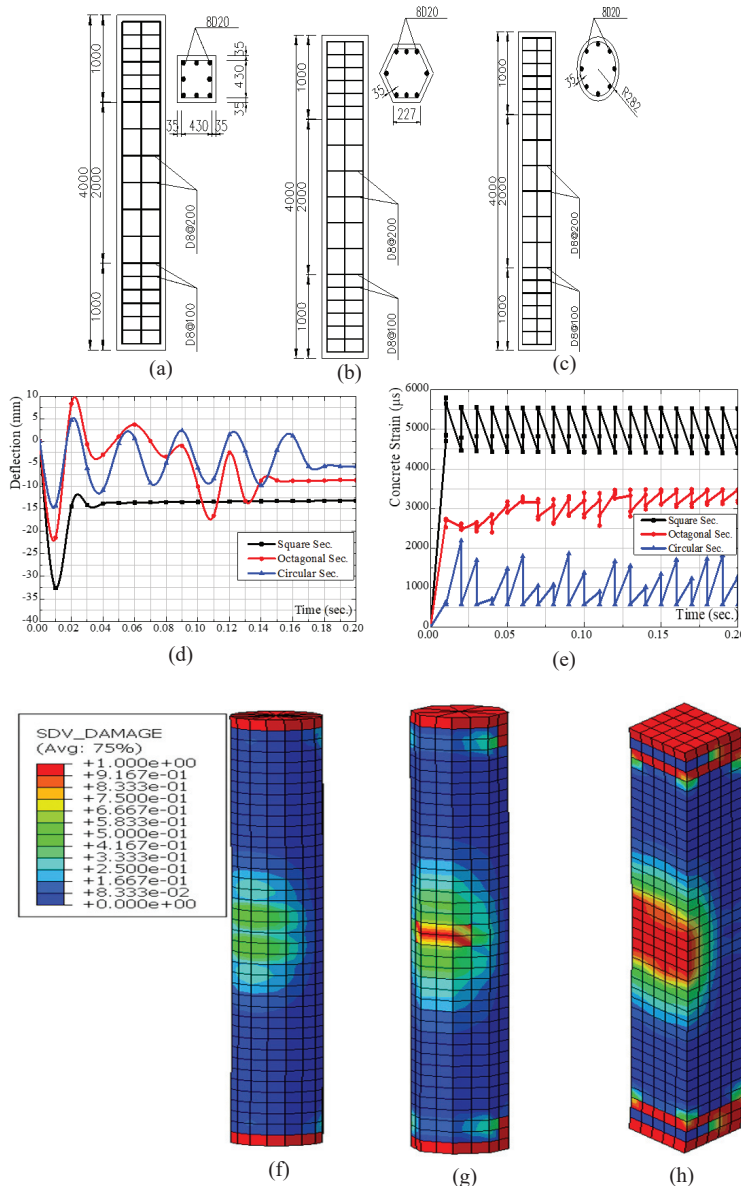


Figure 2. (a, b, c) Detail the columns, (d) Maximum deflection, (e) strain of the UHPC element, and (f), (g), (h) Damage state of UHPC columns with various cross-sections.

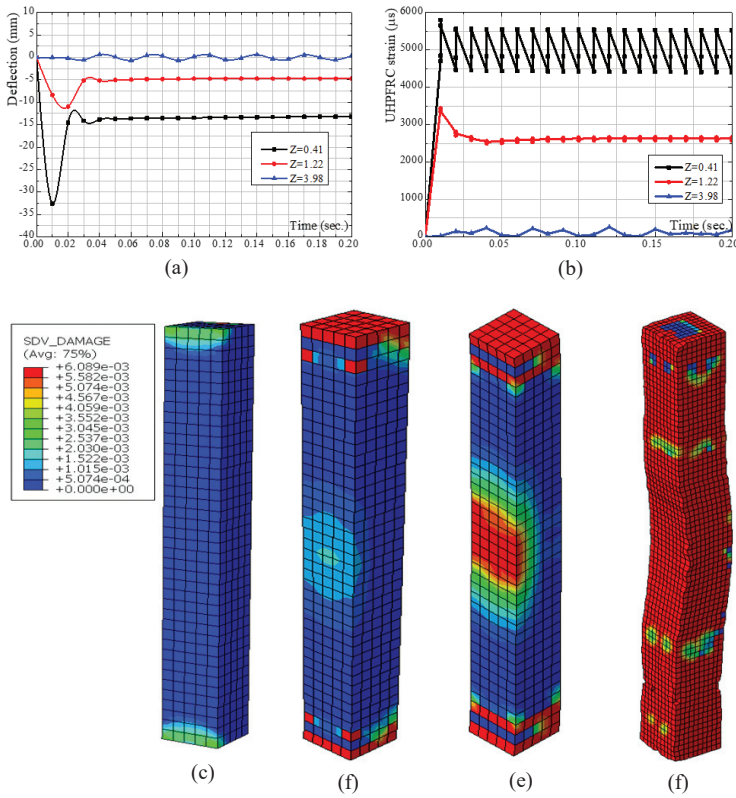


Figure 3. (a) Maximum deflection, (b) Strain of the UHPC element, (c) Damage of column with scaled distances 3.98m/kg^{1/3}, (d) 1.22m/kg^{1/3}, (e) 0.41m/kg^{1/3}, and (f) collapse of column in 0.27m/kg^{1/3}.

a sharp decline in peak deflection as the scaled distance increases. In the far-field regime, maximum deflection of the UHPC column is negligible (0.6 mm). However, there is a considerable increase in deflection when the blast occurs at the near field and close-in regime, corresponding to 11.4 mm and 32.6 mm. The effects of scaled distance on the strain of the UHPC elements are similar to deflection. The maximum strain of the UHPC element is 225.399 µs, 3438.75 µs, and 5801.39 µs for the scaled distances of Z = 3.98 m/kg^{1/3}, 1.22 m/kg^{1/3}, and 0.41 m/kg^{1/3}, respectively.

Figures 3(c), 3(d), 3(e), and Table 4 show the damage state of the UHPC column with various scaled distance. It can be seen that as the scaled distance decreases, the dynamic response of the UHPC column changes. The data reported here appear to support the assumption that the damage state of shear in the far-field regime seems to transform into the state including shear failure and flexural failure when the scaled distance decreases. In the close-in regime, the amount of damage is remarkably larger and more widespread than the

Table 4. Damage state of UHPC column after blast load (percentage by volume)

Z (m/kg ^{1/3})	Light damage	Moderate damage	Severe damage	Collapse
0.27	-	-	-	100%
0.41	14.6%	11.2%	4.8%	//
1.22	8.2%	9.1%	2.5%	//
3.98	5.6%	3.7%	0.6%	//

rest scenarios. Particularly for the scaled distance of 0.27 m/kg^{1/3}, the column is completely collapsed (Fig. 3(f))

3.2.3 Steel Reinforcement Ratio Parameter

This section has reviewed the key aspect of longitudinal reinforcement and lateral reinforcement in the UHPC column subjected to blast loading. Two design scenarios were considered. In the first case, longitudinal reinforcement ratio is increased from 0.8% to 1.6% with the same ratio of lateral reinforcement bar. In the second case, the longitudinal steel bar ratio is kept constant while changing the lateral reinforcement ratio.

In the first case, the maximum deflection and damage state result of the UHPC column with various longitudinal reinforcement ratios are depicted in Fig. 4(a) and Table 5(a). Peak deflection variation is quite small (↑14%), from 29.2 mm for 0.8% of the longitudinal steel ratio to 33.2mm for 1.6% of the longitudinal steel ratio. The longitudinal steel bar does not provide significantly more resistance to the UHPC column under blast load. The damage state and strain of the UHPC column illustrate this point clearly. For instance, severe damage of UHPC column is 5.4%, 4.8%, 3.9% and 3.1% for the steel ratio of 0.8%, 1%, 1.2% and 1.6%, respectively. An increment in the longitudinal reinforcement ratio can significantly increase the bending capacity of the UHPC column, however, it has little contribution to the shear capacity, which plays the important role in the blast resistance capacity of the UHPC column. Taken together, these results suggest that the appropriate ratio of longitudinal steel reinforcement for the UHPC column subjected to serve blast loading might be 1%.

In the second case, the variation of the stirrup in the UHPC column is implemented by increasing the lateral distance. Details of lateral reinforcement in columns C1, C2, and C3 are shown in Figs. 5(a), 5(b), 5(c). Figure 4(b) depicts the shape of deflection curve of the UHPC column. Although there is a significant decrease in lateral reinforcement distribution, the UHPC columns do not exhibit a noticeable increment in peak deflection. Peak deflection of 32.5 mm, 38.2 mm, and 41.5 mm

Table 5. Damage state of UHPC column as: (a) increasing longitudinal steel reinforcement ratio and (b) increasing lateral steel reinforcement distance

(a)				
Longitudinal reinforcement ratio	Light damage	Moderate damage	Severe damage	Collapse
0.8%	16.1%	12.8%	5.4%	//
1%	14.6%	11.2%	4.8%	//
1.2%	13.3%	9.7%	3.9%	//
1.6%	12.4	8.3	3.1%	//

(b)				
Column	Light damage	Moderate damage	Severe damage	Collapse
C1	14.6%	11.2%	4.8%	-
C2	19.5%	18.8%	7.4%	-
C3	25.3%	24.2%	13.4%	-

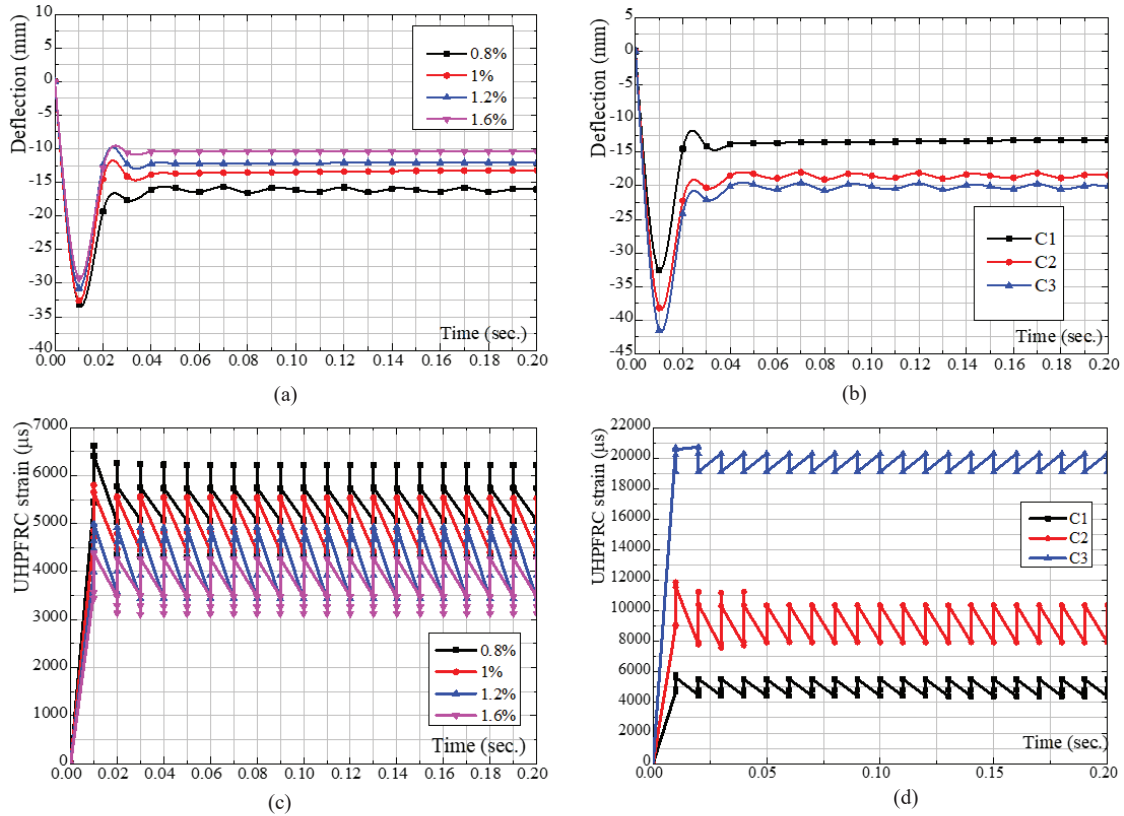


Figure 4. Maximum deflection and strain of the UHPC columns with various steel reinforcement ratio: (a) Longitudinal reinforcement, (b) Lateral reinforcement, (c) Longitudinal reinforcement, and (d) Lateral reinforcement.

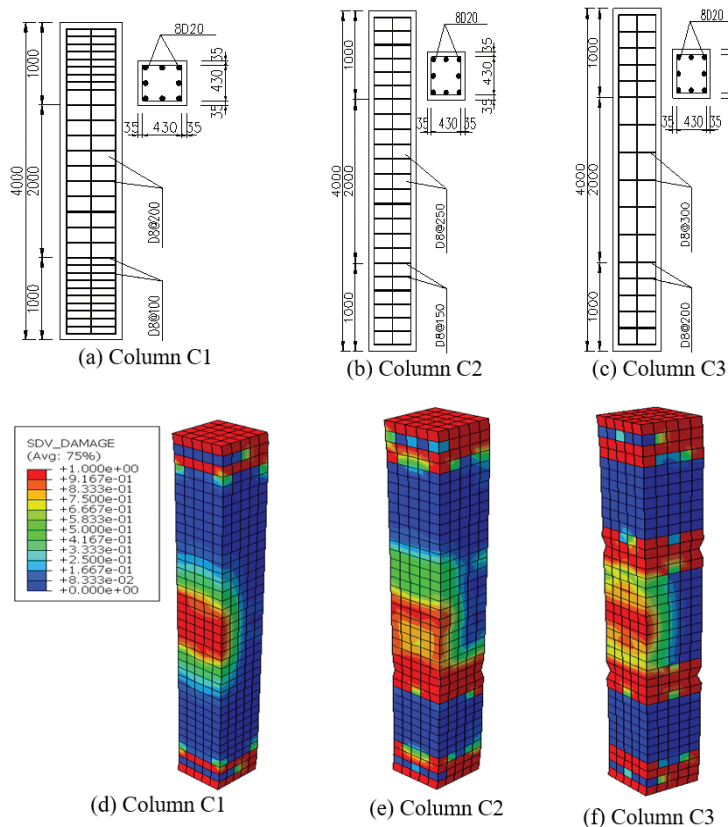


Figure 5. (a, b, c) Distribution of lateral reinforcement and (d, e, f) Damage of UHPC column.

are observed in the column C1, C2, and C3, respectively. However, compared to the first case, the more severe damage state was reported in Figs. 5(d), 5(e), 5(f), and Table 5(b). In column C1, severe damage is 4.8%. The damage variable increases 1.5 times in column C2 (7.4%) and 2.8 times in column C3 (13.4%), respectively. Furthermore, the shrinkage phenomenon of cross-section occurs in the one-third region of column C3. Likewise, concrete strain increases 104 %, from 5801.39 μs of C1 to 11876.5 μs of C2 and 74%, from 11876.5 μs of C2 to 20690.2 μs of C3. Apparently, the lateral reinforcement provides confinement to concrete in the UHPC column to enhance the greater capacity under the effect of an explosion. Compared to the longitudinal reinforcement ratio, the lateral reinforcement ratio affects considerably the ductility and residual resistance of UHPC after blast loading.

3.2.4 Cross-section Area Parameter

Moving on now to consider the effect of area section on the dynamic behaviour of UHPC column under blast loading. Three square columns with a cross-section of 500x500mm, 600× 600mm, 700× 700mm, and 1% steel reinforcement bar ratio are studied under an explosion of 50kG TNT equivalent. Each column is applied to an axial load of 20% load capacity. Maximum deflection, the strain, and damage state of the UHPC column with various cross-section areas are shown in Figs. 6(a), 6(b). The result from this study suggests that both peak deflection, strain, and damage state of the UHPC column decrease as the cross-

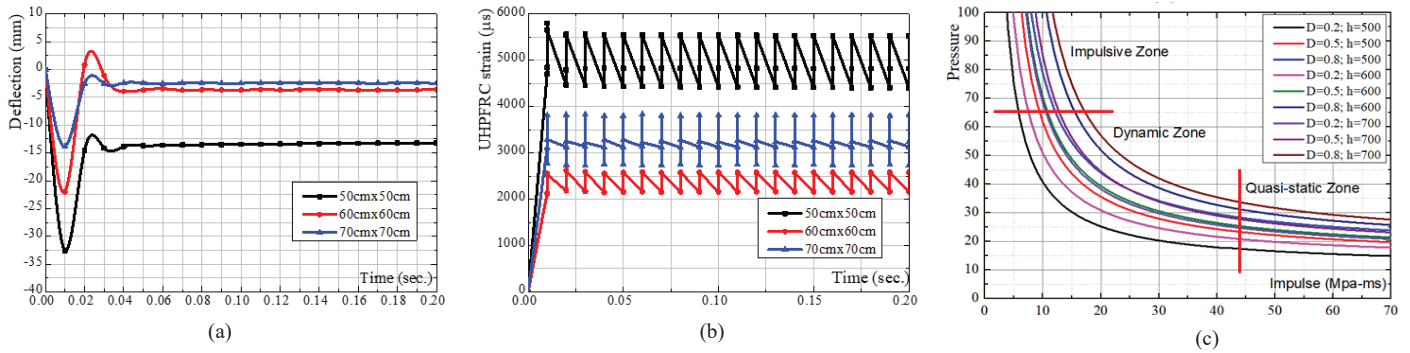


Figure 6. (a) Maximum deflection, (b) Strain of UHPC column, and (c) P-I diagram with different damage constants against cross-section area.

section area of the column increases. An increment in the cross-section can significantly increase the blast loading resistance capacity of the UHPC column.

P-I diagram plays an important role in analysing quickly the damage of the UHPC column under blast loading, which includes a series of damage curves with different damage levels. In the present study, the residual loading capacity of the UHPC column is calculated for three damage levels of 20%, 50%, and 80%. According to Shi³⁴, *et al.*, the pressure-impulse (P-I) curves can be expressed as:

$$(P - P_0)(I - I_0) = 12(P_0 / 2 + I_0 / 2)^{1.5} \quad (9)$$

where: P_0 denotes the pressure asymptote for individual damage level D . In the present study, D is applied as 0.2, 0.5, and 0.8. I_0 represents the impulsive asymptote for individual damage level. Value of P_0 and I_0 with different damage levels and cross-section areas of the UHPC column can be extracted from the simulation result. Table 6 summarises the parameters of pressure and impulsive asymptotes depending on the cross-section area of the UHPC column. Substituting P_0 and I_0 from Table 6 into Eqn (9) for each case, the P-I curve is defined. Consequently, the combination of the P-I diagram representing three damage levels, that is, 20%, 50%, and 80% against the cross-section area is obtained as in Fig. 6. P-I curve identifies three domains, including an impulsive zone, dynamic zone, and a quasi-static zone. The impulsive zone is characterised by short load duration, where the column tends to be failed under shear. The quasi-static zone consists of the state that the column is prone to be damaged by flexural failure. The dynamic zone is characterised by the maximum response being reached close to the end of the loading regime, having a combination of shear and flexure failure. Base on the P-I diagram, one see that both pressure and impulsive asymptote increase as the column size increase. Although increasing the cross-section area, impulsive and capacity of the UHPC column increase, however, blast resistance of the UHPC column overweights the increment in the blast loading.

4. CONCLUSIONS

The paper presented the results obtained from the simulation model of 20 UHPC columns subjected to blast loading using a subroutine, which is integrated with ABAQUS software associated with the unique material model of UHPC. The following conclusions are drawn:

Table 6. Pressure and impulsive asymptotes with different cross-section area of UHPC column

Column height (h)	D=0.2		D=0.5		D=0.8	
	P_0 (MPa)	I_0 (MPa.ms)	P_0 (MPa)	I_0 (MPa.ms)	P_0 (MPa)	I_0 (MPa.ms)
50cmx50cm	5.7	10.8	6.7	13.9	7.1	16.6
60cmx60cm	5.9	12.8	7.1	14.9	8.7	18.2
70cmx70cm	7.3	14.5	7.9	15.8	9.2	19.3

- With the same area, compared to various cross-sections of UHPC column under high explosion, square column suffers the largest deformation and most serious damage. On the contrary, the UHPC circular column shows the greatest capacity to resist blast loading and should be considered in the blast-resistant design.
- The authors propose the longitudinal steel reinforcement ratio of 1% for the UHPC column subjected to blast loading. Increasing the longitudinal steel reinforcement ratio does not show a significant effect on the blast loading resistance of the UHPC column. Ductility and residual resistance of the UHPC column after the blast considerably affected by the steel lateral reinforcement ratio.
- As increasing the cross-section area, the blast loading resistance capacity of the UHPC column is strengthened significantly. Based on the numerical results, the pressure - impulsive (PI) diagram can be defined to quickly predict the damage of the UHPC column under blast loading.

REFERENCES

1. Ngo, T; Mendis, P; Gupta, A; Ramsay, J. Blast loading and blast effects on structures - An overview. *Electron. J. Struct. Eng.*, 2007, **7**, 76-91.
2. Abbas, A; Adil, M; Ahmad, N; Ahmad, I. Behavior of reinforced concrete sandwiched panels (RCSPs) under blast load. *Eng. Struct.*, 2019, **181**, 476-490. doi: 10.1016/j.engstruct.2018.12.051
3. Li, J; Wu, C; Hao, H; Su, Y. Investigation of ultra-high performance concrete under static and blast loads. *Int. J. Prot. Struct.*, 2015, **6**(2), 217-234. doi: 10.1260/2041-4196.6.2.217
4. Mai, VC; Nguyen, TC; Dao, CB. Numerical simulation

- of ultra-high-performance fiber-reinforced concrete frame structure under fire action. *Asian J. Civ. Eng.*, 2020, **21**(5), 797-804.
doi: 10.1007/s42107-020-00240-4
5. Shaikh, FUA; Luhar, S; Arel, HŞ; Luhar, I. Performance evaluation of Ultrahigh performance fibre reinforced concrete - A review. *Constr Build Mater.*, 2020, **232**.
doi: 10.1016/j.conbuildmat.2019.117152
 6. Yujing, L; Wenhua, Z; Fan, W; Peipei, W; Weizhao, Z; Fenghao, Y. Static mechanical properties and mechanism of C200 ultra-high performance concrete (UHPC) containing coarse aggregates. *Sci. Eng. Composite Mater.*, 2020, **27**(1), 186-195.
doi: 10.1515/secm-2020-0018
 7. Tawfik, TA; El-Yamani, MA; Abd El-Aleem, S; Serag Gabr, A; Abd El-Hafez, GM. Effect of nano-silica and nano-waste material on durability and corrosion rate of steel reinforcement embedded in high-performance concrete. *Asian J. Civil Eng.*, 2019, **20**(1), 135-147.
doi: 10.1007/s42107-018-0093-5
 8. Wang, JY; Bian, C; Xiao, RC; Ma, B. Restrained Shrinkage Mechanism of Ultra High Performance Concrete. *KSCE J. Civ. Eng.*, 2019, **23**(10), 4481-4492.
doi: 10.1007/s12205-019-0387-5
 9. Azmee, NM; Shafiq, N. Ultra-high performance concrete: From fundamental to applications. *Case Stud. Constr. Mater.*, 2018; **9**.
doi: 10.1016/j.cscm.2018.e00197
 10. Murali, G; Venkatesh, J; Lokesh, N; Nava, TR; Karthikeyan, K. Comparative Experimental and Analytical Modeling of Impact Energy Dissipation of Ultra-High Performance Fibre Reinforced Concrete. *KSCE J. Civ. Eng.*, 2018, **22**(8), 3112-3119.
doi: 10.1007/s12205-017-1678-3
 11. Wang, Z; Wang, J; Liu, T; Zhang, F. Modeling seismic performance of high-strength steel-ultra-high-performance concrete piers with modified Kent-Park model using fiber elements. *Adv. Mech. Eng.*, 2016, **8**(2), 1-14.
doi: 10.1177/1687814016633411
 12. Fan, P; Wang, M; Song, C. Anti-strike Capability of Steel-fiber Reactive Powder Concrete. *Def. Sci. J.*, 2013, **63**(4), 363-368.
doi: 10.14429/dsj.63.2407
 13. Mai, V-C. Assessment of Dynamic Response of 3D Ultra High Performance Concrete Frame Structure under High Explosion Using Johnson-Holmquist 2 Model. *KSCE J. Civ. Eng.*, 2020, 1-11.
doi: 10.1007/s12205-020-1373-7
 14. Fujikura, S; Bruneau, M. Experimental investigation of seismically resistant bridge piers under blast loading. *J. Bridge Eng.*, 2011, **16**(1), 63-71.
doi: 10.1061/(ASCE)BE.1943-5592.0000124
 15. Williamson, EB; Bayrak, O; Davis, C; Williams, GD. Performance of bridge columns subjected to blast loads. I: Experimental program. *J. Bridge Eng.*, 2011, **16**(6), 693-702.
doi: 10.1061/(ASCE)BE.1943-5592.0000220
 16. Li, Z; Zhong, B; Shi, Y. An effective model for analysis of reinforced concrete members and structures under blast loading. *Adv. Struct. Eng.*, 2016, **19**(12), 1815-1831.
doi: 10.1177/1369433216649393
 17. Esmailnia Omran, M; Mollaei, S. Investigation of Axial Strengthened Reinforced Concrete Columns under Lateral Blast Loading. *Shock. Vib.*, 2017, **2017**(2010).
doi: 10.1155/2017/3252543
 18. Liu, Y; Yan, J bo; Huang, F lei. Behavior of reinforced concrete beams and columns subjected to blast loading. *Def. Technol.*, 2018, **14**(5), 550-559.
doi: 10.1016/j.dt.2018.07.026
 19. Thai, DK; Pham, TH; Nguyen, DL. Damage assessment of reinforced concrete columns retrofitted by steel jacket under blast loading. *Struct. Des. Tall Spec. Build.*, 2020, **29**(1), 1-15.
doi: 10.1002/tal.1676
 20. Astarlioglu, S; Krauthammer, T. Response of normal-strength and ultra-high-performance fiber-reinforced concrete columns to idealized blast loads. *Eng. Struct.*, 2014, **61**, 1-12.
doi: 10.1016/j.engstruct.2014.01.015
 21. Aoude, H; Dagenais, FP; Burrell, RP; Saatcioglu, M. Behavior of ultra-high performance fiber reinforced concrete columns under blast loading. *Int. J. Impact Eng.*, 2015, **80**, 185-202.
doi: 10.1016/j.ijimpeng.2015.02.006
 22. Su, Y; Li, J; Wu, C; Wu, P; Li, ZX. Influences of nano-particles on dynamic strength of ultra-high performance concrete. *Compos. B. Eng.*, 2016, **91**, 595-609.
doi: 10.1016/j.compositesb.2016.01.044
 23. Holmquist, TJ; Johnson, GR; Cook, WH. A Computational Constitutive Model for Concrete Subjected to Large Strains, High Strain Rates and High Pressures. *14th International symposium, Warhead mechanisms, terminal ballistics*, 1993, **2**, 591-600.
 24. Johnson, G.R. & Holmquist, T.J. A computational constitutive model for brittle materials subjected to large strains, high strain rates and high pressures. *Shock Wave and High Strain Rate Phenomena in Materials, CRC Press: Boca Raton, FL, USA*, 1992, (1), 1075-1081.
 25. Mao, L; Barnett, S; Begg, D; Schleyer, G; Wight, G. Numerical simulation of ultra high performance fibre reinforced concrete panel subjected to blast loading. *Int. J. Impact Eng.*, 2014; **64**, 91-100.
doi: 10.1016/j.ijimpeng.2013.10.003
 26. Mai, V-C; Vu, N-Q; Pham, H; Nguyen, V-T. Ultra-High Performance Fiber Reinforced Concrete Panel Subjected to Severe Blast Loading. *Def. Sci. J.*, 2020, **70**(6), 603-611.
doi: 10.14429/dsj.70.15835
 27. Xu, J; Wu, C; Xiang, H; et al. Behaviour of ultra high performance fibre reinforced concrete columns subjected to blast loading. *Eng. Struct.*, 2016, **118**, 97-107.
doi: 10.1016/j.engstruct.2016.03.048
 28. Yu, R; Spiesz, P; Brouwers, HJH. Numerical simulation of ultra-high performance fibre reinforced concrete (UHPFRC) under high velocity impact of deformable projectile. *Distribution A: For Public Release*, 2013, 1-10.

29. Nordendale, NA. Modeling and simulation of brittle armours under impact and blast effects. 2013, 166.
30. David W Hyde. User's Guide for Microcomputer Programs ConWep and FunPro, Applications of TM 5-855-1: Fundamentals of Protective Design for Conventional Weapons. Vicksburg, Miss. : U.S. Army Engineer Waterways Experiment Station; 1988.
31. Prueter, PE. Using Explicit Finite Element Analysis to Simulate Blast Loading on Hazardous Chemical Storage Tanks. , 1-15.
32. Hallquist, JO; Wainscott, B; Schweizerhof, K. Improved simulation of thin-sheet metalforming using LS-DyNA3D on parallel computers. *J. Mater. Process. Technol.*, 1995, **50**(1-4), 144-157.
doi: 10.1016/0924-0136(94)01376-C
33. M. Smith, S., McCann, D and K. Blast Resistant Design Guide for Reinforced Concrete Structures. Portland Cement Association; 2009.
34. Shi, Y; Hao, H; Li, ZX. Numerical derivation of pressure-impulse diagrams for prediction of RC column damage to blast loads. *Int. J. Impact Eng.*, 2008, **35**(11), 1213-1227.
doi: 10.1016/j.ijimpeng.2007.09.001

CONTRIBUTORS

Mr Viet-Chinh Mai is a PhD student at Department of Civil Engineering, Kumoh National Institute of Technology, South Korea. His research work involves the Ultra High Performance Concrete, steel, and composite structure.

In the current study, he conceived the original idea, performed the analytic calculations, and performed the numerical simulations.

Mr Xuan-Bach Luu is a PhD student at Department of Civil Engineering, Kumoh National Institute of Technology, South Korea. His research area consists of concrete structure, finite element modelling, artificial intelligence.

In this study, he contributed to the interpretation of the results, provided critical feedback, and helped shape the research, analysis, and manuscript.

Dr Cong-Binh Dao is working as a senior lecturer and researcher at Dept. of Civil Engineering, Le Quy Don Technical University.

He is interested in structural engineering, including concrete structure, steel structure, and composite structure.

He supervised the results of this work, wrote the manuscript in consultation with other authors.

Mr Dinh-Viet Le is pursuing a PhD at Department of Civil Environmental and Railroad Engineering, PaiChai University, South Korea. His research work involves railway structure, geotechnics, and programming language.

In this study, he worked out the issues of the study and contributed to the final version of the manuscript.